LETTER

doi:10.1038/nature10486

Inhibition of miR-33a/b in non-human primates raises plasma HDL and lowers VLDL triglycerides

Katey J. Rayner[1], Christine C. Esau[2], Farah N. Hussain[1], Allison L. McDaniel[3], Stephanie M. Marshall[3], Janine M. van Gils[1], Tathagat D. Ray[1], Frederick J. Sheedy[1], Leigh Goedeke[1], Xueqing Liu[2], Oleg G. Khatsenko[2], Vivek Kaimal[2], Cynthia J. Lees[4], Carlos Fernandez-Hernando[1], Edward A. Fisher[1], Ryan E. Temel[3]* & Kathryn J. Moore[1]*

Cardiovascular disease remains the leading cause of mortality in westernized countries, despite optimum medical therapy to reduce the levels of low-density lipoprotein (LDL)-associated cholesterol. The pursuit of novel therapies to target the residual risk has focused on raising the levels of high-density lipoprotein (HDL)-associated cholesterol in order to exploit its atheroprotective effects[1]. MicroRNAs (miRNAs) have emerged as important post-transcriptional regulators of lipid metabolism and are thus a new class of target for therapeutic intervention[2]. MicroRNA-33a and microRNA-33b (miR-33a/b) are intronic miRNAs whose encoding regions are embedded in the sterol-response-element-binding protein genes *SREBF2* and *SREBF1* (refs 3–5), respectively. These miRNAs repress expression of the cholesterol transporter ABCA1, which is a key regulator of HDL biogenesis. Recent studies in mice suggest that antagonizing miR-33a may be an effective strategy for raising plasma HDL levels[3–5] and providing protection against atherosclerosis[6]; however, extrapolating these findings to humans is complicated by the fact that mice lack miR-33b, which is present only in the *SREBF1* gene of medium and large mammals. Here we show in African green monkeys that systemic delivery of an anti-miRNA oligonucleotide that targets both miR-33a and miR-33b increased hepatic expression of ABCA1 and induced a sustained increase in plasma HDL levels over 12 weeks. Notably, miR-33 antagonism in this non-human primate model also increased the expression of miR-33 target genes involved in fatty acid oxidation (*CROT*, *CPT1A*, *HADHB* and *PRKAA1*) and reduced the expression of genes involved in fatty acid synthesis (*SREBF1*, *FASN*, *ACLY* and *ACACA*), resulting in a marked suppression of the plasma levels of very-low-density lipoprotein (VLDL)-associated triglycerides, a finding that has not previously been observed in mice. These data establish, in a model that is highly relevant to humans, that pharmacological inhibition of miR-33a and miR-33b is a promising therapeutic strategy to raise plasma HDL and lower VLDL triglyceride levels for the treatment of dyslipidaemias that increase cardiovascular disease risk.

Recent advances in the understanding of lipid metabolism have revealed that the genetic loci encoding the transcription factors SREBP1 and SREBP2 (known as *SREBF1* and *SREBF2*) also encode the miRNAs miR-33b and miR-33a, respectively, which regulate cholesterol and fatty acid homeostasis together with their host genes[3–5,7–9]. Although miR-33a and miR-33b differ by two nucleotides in their mature form, they are identical in their seed sequence and thus are predicted to repress the same subset of genes. Notably, miR-33a has been highly conserved throughout evolution, whereas miR-33b is encoded only by the *SREBF1* gene of medium and large mammals. This difference between mice and humans may be particularly relevant under conditions in which the transcription of *SREBF1*, and thus miR-33b, is highly upregulated, such as insulin resistance[9]. Recently, we and others have reported that the silencing of mature miR-33a in mice, by using modified antisense oligonucleotides[4,6], by viral delivery of hairpin inhibitors[3,5] or by targeted deletion of the miR-33-encoding locus[10], increased the levels of hepatic ABCA1 and circulating HDL by as much as 40%. Although these studies highlight the therapeutic promise of miR-33 inhibitors for raising plasma HDL levels, the absence of miR-33b in mice limits the translational relevance of these findings.

Thus, to gain a comprehensive understanding of the effects of inhibiting both miR-33a and miR-33b in a model highly related to humans, we treated African green monkeys (*Chlorocebus aethiops*) with a 2′-fluoro/methoxyethyl (2′-F/MOE)-modified, phosphorothioate-backbone-modified, antisense miR33 (denoted anti-miR33), which we showed was equally effective at inhibiting both miR-33a and miR-33b *in vitro* (Supplementary Fig. 1a). Six animals per group were subcutaneously administered a clinically relevant dose of anti-miR-33 (5 mg kg^{-1}) or a mismatch control[11] twice weekly for the first two weeks and then weekly for the remainder of the study (Fig. 1a). Quantification of hepatic anti-miRNA levels by ion-pairing high-performance liquid chromatography (HPLC) coupled to electrospray mass spectrometry (ES/MS) after 4 and 12 weeks of treatment showed equivalent delivery of anti-miR-33 and control (mismatch) oligonucleotides (Supplementary Fig. 1b). No toxicity seemed to be associated with the anti-miRNA treatment, as shown by the clinical chemistries, blood counts, coagulation markers, body weights and serum cytokine profiles of the monkeys (Fig. 1b and Supplementary Fig. 1c, d), which remained within normal limits throughout the study.

Microarray profiling of messenger RNA obtained from liver biopsies after 4 weeks of treatment revealed that anti-miR-33 selectively increased the expression of miR-33 heptamer-matched genes in monkeys fed a normal chow diet (Supplementary Table 1). Of these, the gene encoding the cholesterol transporter ABCA1 was the most highly derepressed miR-33 target gene. Reverse transcription followed by quantitative PCR (RT–qPCR) analysis confirmed the increase in *ABCA1* expression, as well as that of other known miR-33 target genes (target site alignment is shown in Supplementary Fig. 2), including the genes encoding two enzymes involved in fatty acid oxidation, *CROT* and *HADHB,* and the insulin signalling gene *IRS2* (Fig. 1c and Supplementary Fig. 3).

To assess the effects of miR-33 inhibition under different metabolic conditions, monkeys were switched after 4 weeks to a high carbohydrate, moderate cholesterol diet for 8 weeks, thereby totalling 12 weeks of treatment. After 8 weeks of the high carbohydrate, moderate cholesterol diet, *SREBF1* mRNA levels increased by 5-fold in the control animals, and a corresponding 2.2-fold increase in miR-33b was observed, making its expression more than 7-fold higher than miR-33a (Fig. 1d and Supplementary Fig. 3). Microarray and RT–qPCR analysis showed that

[1]Marc and Ruti Bell Vascular Biology and Disease Program, Leon H. Charney Division of Cardiology, Department of Medicine, New York University School of Medicine, New York, New York 10016, USA. [2]Regulus Therapeutics, San Diego, California 92121, USA. [3]Department of Pathology-Section on Lipid Sciences, Wake Forest University School of Medicine, Winston-Salem, North Carolina 27157, USA. [4]Department of Pathology-Section on Comparative Medicine, Wake Forest University School of Medicine, Winston-Salem, North Carolina 27157, USA.
*These authors contributed equally to this work.

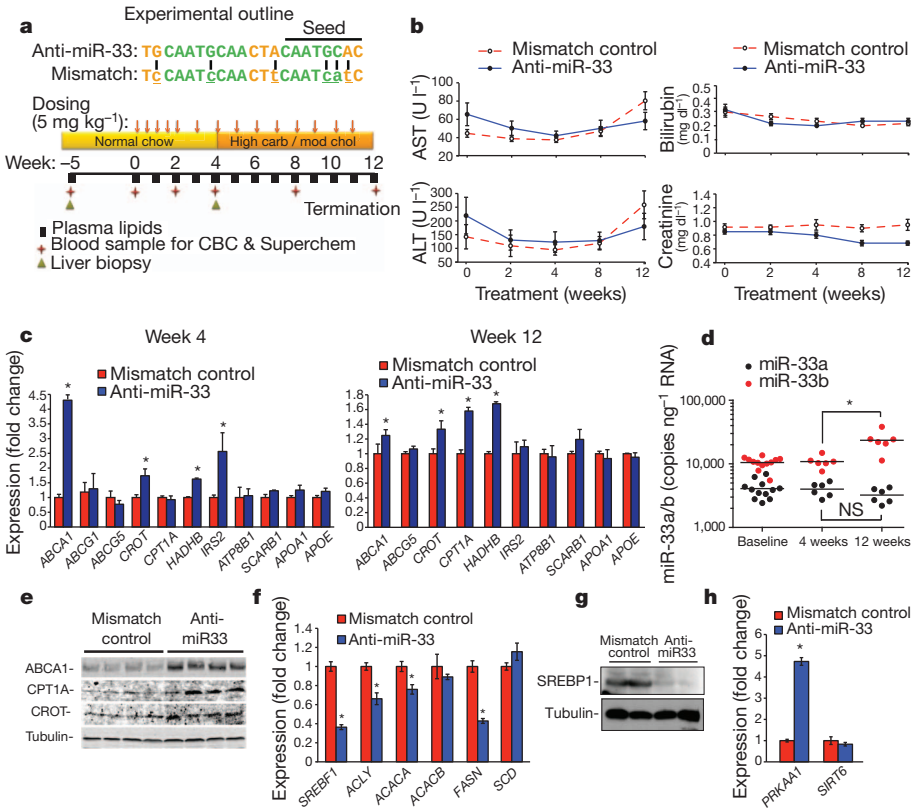

Figure 1 | Silencing of miR-33a/b in non-human primates. **a**, Experimental outline of anti-miR33 or mismatch control oligonucleotide treatment of African green monkeys ($n = 6$ per group). High carb / mod chol, high carbohydrate, moderate cholesterol diet. **b**, Serum transaminase (AST and ALT), bilirubin and creatinine levels. **c**, Hepatic gene expression in anti-miRNA-treated monkeys fed a chow diet (at week 4) or a high carbohydrate, moderate cholesterol diet (at week 12). **d**, Quantification of miR-33a and miR-33b levels in anti-miRNA-treated monkeys. **e**, Western blot for hepatic ABCA1, CPT1A and CROT following 12 weeks of anti-miRNA treatment. **f**, Expression of hepatic *SREBF1* mRNA and its downstream genes after 12 weeks of anti-miRNA treatment. SCD, stearoyl-CoA desaturase. **g**, SREBP1 protein after 12 weeks of anti-miRNA treatment. **h**, Hepatic *PRKAA1* and *SIRT6* mRNA after 12 weeks of anti-miRNA treatment. Data are presented as the mean ± s.e.m. *, $P \leq 0.05$.

the derepression of the above-mentioned miR-33 target genes by anti-miR-33 was largely sustained in monkeys fed a high carbohydrate, moderate cholesterol diet (Fig. 1c, Supplementary Fig. 3 and Supplementary Table 2). Under these diet conditions, we observed an increase in an additional miR-33 target gene involved in fatty acid oxidation, *CPT1A* (Fig. 1c and Supplementary Fig. 3). Although *ABCG5* and *ATP8B1* are predicted to contain miR-33-binding sites, no difference in their mRNA levels was observed (Fig. 1c). Furthermore, throughout the study we observed no difference between the groups in the expression of hepatic lipid metabolism genes lacking miR-33-binding sites, such as *APOE* and *APOA1*, or in *ABCG1*, which lacks the miR-33-binding site present in the mouse gene (Fig. 1c and Supplementary Fig. 3). Marked upregulation of *ABCA1* mRNA in anti-miR-33-treated monkeys was also observed in the spleen, which is a macrophage-rich tissue (Supplementary Fig. 1f).

As miRNAs can affect both mRNA stability and translation, we measured hepatic ABCA1, CROT and CPT1A protein levels after 4 weeks of chow diet treatment. All three of these miR-33 targets were present in increased amounts in the livers of monkeys that had been treated with anti-miR-33 compared to monkeys treated with mismatch control (Supplementary Fig. 1e). Furthermore, despite anti-miR-33 having only modest effects on the amount of *ABCA1* mRNA after 12 weeks of treatment, hepatic ABCA1 protein levels remained robustly increased, as did the expression of CROT and CPT1A (Fig. 1e).

Notably, although we observed no difference in *SREBF2* expression in anti-miR-33-treated or control anti-miRNA-treated animals over the course of the study, we detected a 50% decrease in *SREBF1* mRNA in the anti-miR-33-treated monkeys at 12 weeks (Fig. 1f and Supplementary Fig. 3), which was confirmed by western blotting (Fig. 1g). We postulated that this decrease in SREBP1 may result from the derepression of negative regulators of this pathway that are targeted by miR-33. Consistent with this hypothesis, we observed a fourfold increase in AMP-activated protein kinase (*PRKAA1*) mRNA in the livers of anti-miR-33-treated monkeys, whereas no change in sirtuin 6 (*SIRT6*) mRNA was detected (Fig. 1h). SREBP1 has a major role in the transcriptional regulation of fatty acid synthesis, and measurement of its downstream target genes revealed decreased mRNA levels of ATP citrate lyase (*ACLY*), acetyl-CoA carboxylase-α (*ACACA*) and fatty acid synthase (*FASN*) (Fig. 1f).

As increased hepatic expression of ABCA1 would be predicted to augment HDL biogenesis, we measured plasma lipoprotein cholesterol levels. Whereas weekly blood sampling revealed no difference in total plasma cholesterol or LDL-associated cholesterol between treatment groups, there was both a significant decrease in VLDL-associated cholesterol and an increase in HDL-associated cholesterol in anti-miR-33-treated monkeys compared with mismatch-control-treated monkeys (Fig. 2a–d). A maximal HDL increase of 50% was reached after 8 weeks and was sustained throughout the remainder of the study (Fig. 2b). Correspondingly, lipoprotein separation by fast protein liquid chromatography (FPLC) showed increased cholesterol in the HDL fraction and a left-shifted HDL peak in anti-miR-33-treated monkeys compared with mismatch-control-treated monkeys, suggesting the presence of larger HDL particles (Fig. 2e).

To characterize further the HDL, we examined the plasma concentrations of apolipoprotein AI (apoAI), apoAII and apoE both in total plasma and in HDL fractionated by FPLC, by using enzyme-linked immunosorbent assays (ELISAs) and western blotting, respectively. By these two measures, we observed that anti-miR-33-treated monkeys had significant increases in the amounts of the primary apolipoproteins carried on HDL—that is, apoAI and apoAII—associated with large and very large HDL particles compared with mismatch-control-treated monkeys (Fig. 3a, b and Supplementary Fig. 4). As the static measurement of HDL has inherent limitations in extrapolating to its functionality[1], we examined the atheroprotective properties of anti-miR-33-generated HDL, namely its ability to promote cholesterol efflux by macrophages and to protect endothelial cells from cytokine-induced inflammation. Equivalent volumes of serum or polyethylene glycol (PEG)-isolated HDL from anti-miR-33-treated monkeys induced greater macrophage cholesterol efflux than did the same volumes from control monkeys (Fig. 3c), correlating with the plasma

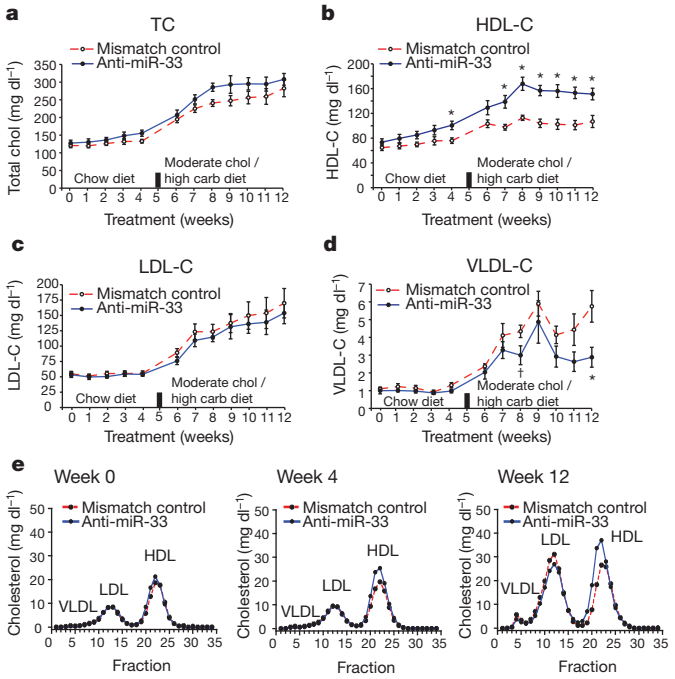

Figure 2 | Plasma cholesterol levels in control-treated and anti-miR33-treated monkeys. **a**–**d**, Levels of total cholesterol (TC) (**a**), HDL cholesterol (HDL-C) (**b**), LDL cholesterol (LDL-C) (**c**) and VLDL cholesterol (VLDL-C) (**d**) in the plasma of monkeys treated with anti-miR-33 or mismatch control. *, $P \leq 0.05$; †, $P \leq 0.1$. **e**, Cholesterol content of FPLC-fractionated lipoproteins. Data are presented as the mean ± s.e.m.

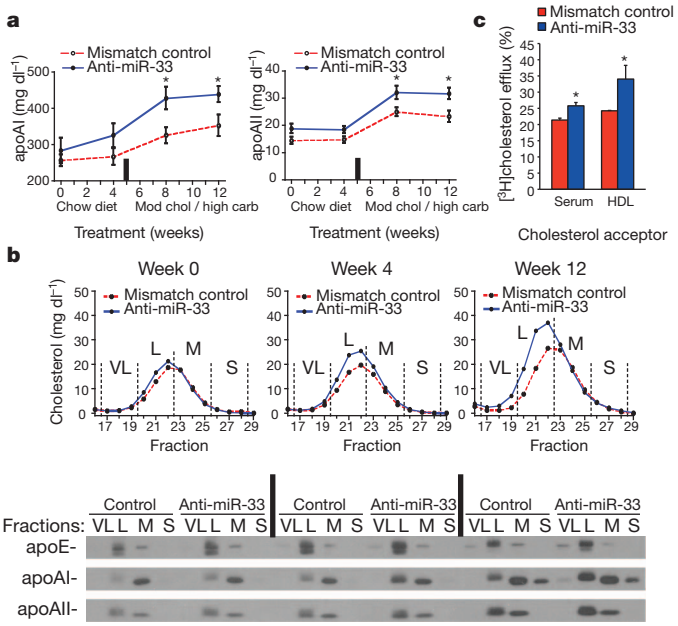

Figure 3 | Characterization of HDL. **a**, Plasma apoAI and apoAII in monkeys treated with anti-miR-33 or mismatch control. *, $P \leq 0.05$. Mod chol / high carb, high carbohydrate, moderate cholesterol diet. **b**, HDL fractions obtained from FPLC fractionation of plasma (top) analysed by western blotting (bottom) for apoE, apoAI and apoAII. L, large particles; M, medium particles; S, small particles; VL, very large particles. **c**, Macrophage cholesterol efflux into serum (2.5%) or PEG-isolated HDL from monkeys treated with anti-miR-33 or mismatch control. *, $P \leq 0.05$. Data are presented as the mean ± s.e.m.

HDL concentration in these animals. When normalized for cholesterol content, the PEG-isolated HDL from anti-miR-33-treated and control-treated monkeys showed similar acceptor capacity for cholesterol efflux from macrophages (data not shown). Furthermore, anti-miR-33-generated HDL maintained its anti-inflammatory effects on endothelial cells (Supplementary Fig. 4).

Given the reciprocal effects of anti-miR-33 treatment on the expression of genes involved in fatty acid oxidation and synthesis, we next measured plasma triglyceride levels. In anti-miR-33-treated monkeys, there was a striking reduction in plasma triglyceride levels compared with control-treated monkeys (Fig. 4a). This decrease was apparent as early as 4 weeks and reached a maximum reduction of 50% at the termination of the study. Fractionation of plasma lipoproteins revealed that this decrease derived primarily from a reduced level of VLDL triglycerides throughout the study and a decrease in LDL triglycerides at 12 weeks (Fig. 4b). VLDL particle analysis by NMR spectroscopy showed a decreased accumulation of large VLDL particles in anti-miR-33-treated monkeys compared with control-treated monkeys (Fig. 4c), with a corresponding decrease in apoB and apoE in the VLDL fraction (Fig. 4d). Thus, by simultaneously increasing fatty acid oxidation by derepression of *HADHB*, *CPT1A* and *CROT* and decreasing fatty acid synthesis by inhibition of the SREBP1 pathway, anti-miR-33 treatment leads to a pronounced reduction in plasma VLDL triglycerides.

The development of novel therapies to exploit the atheroprotective properties of HDL is an area of intense investigation[1]. In randomized clinical trials, raising plasma HDL concentrations by augmenting apoAI levels or by treating with niacin has shown direct benefits in patients with coronary artery disease, including reducing cardiovascular event rates and plaque volume[1,12]. However, the development of HDL-raising drugs has proven particularly challenging[12]. Previous studies by our group and others have shown that inhibiting mature miR-33a in mice is an effective strategy to raise HDL levels[3–5] and to enhance reverse cholesterol transport and induce the regression of atherosclerotic plaques[6]. Although promising, these studies in mice can provide only limited translational insight because mice lack miR-33b expression, which may contribute substantially to miR-33 levels in humans.

This study in non-human primates is the first to show that inhibiting both miR-33a and miR-33b has a profound and sustained effect on circulating HDL levels. Importantly, this study also establishes that miR-33 antagonism markedly suppresses plasma VLDL triglyceride levels, partly as a result of regulating key genes involved in fatty acid oxidation[7,8] and synthesis. Because low HDL levels and high VLDL triglyceride levels are commonly associated with metabolic syndrome[13], miR-33 inhibitors may have clinical utility for the treatment of this growing health concern. Notably, as was recently reported

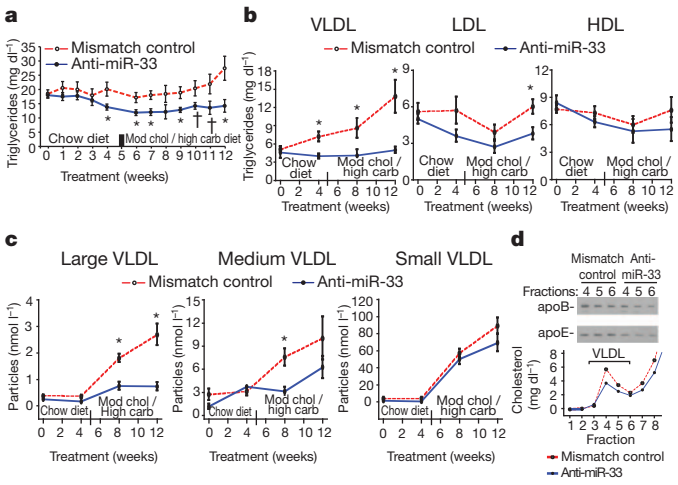

Figure 4 | Triglyceride and VLDL particle analysis. **a**, **b**, Level of total triglycerides (**a**), VLDL triglycerides, LDL triglycerides or HDL triglycerides (**b**) in the plasma of monkeys treated with anti-miR-33 or mismatch control. *, $P \leq 0.05$; †, $P \leq 0.1$. **c**, Quantification of the concentration of small, medium and large VLDL particles by NMR spectroscopy. *, $P \leq 0.05$. **d**, Western blot (top) of apoE and apoB in VLDL fractions (bottom) obtained from FPLC fractionation of plasma. Data are presented as the mean ± s.e.m.

in mice[7], the inhibition of miR-33 in monkeys also increased hepatic expression of *IRS2*, a key component of insulin signalling, which also becomes dysfunctional in individuals with metabolic syndrome[13]. As the monkeys used in this study were normoglycaemic, future studies in primate models of obesity and diabetes will be important to test the effects of miR-33 inhibition on insulin signalling.

Taken together, our findings show that pharmacological inhibition of miR-33a and miR-33b leads to a sustained increase in plasma HDL cholesterol and a coincident decrease in VLDL triglycerides without any evidence of adverse effects. These findings in non-human primates support the development of antagonists of miR-33 as potential therapeutics for dyslipidaemia, atherosclerosis and related metabolic diseases.

METHODS SUMMARY

All experiments were performed in accordance with National Institutes of Health guidelines for animal research and were approved by the Wake Forest University Health Science Institutional Animal Care and Use Committee. Male African green monkeys ($n = 6$ per group) were injected subcutaneously with 5 mg kg^{-1} 2′-F/MOE antisense miR-33 or mismatch anti-miRNA (Regulus Therapeutics) twice weekly for 2 weeks and then weekly until the termination of the study. Monkeys were fed a weighed amount of chow or a high carbohydrate, moderate cholesterol semisynthetic diet. Serum and whole blood samples were analysed using Superchem and CBC tests (ANTECH Diagnostics), respectively. Plasma lipoprotein cholesterol and triglyceride distribution were determined by online gel-filtration HPLC. Pooled plasma was separated by FPLC on a Superose 6 10/300 GL column (GE Healthcare). Plasma lipoprotein particle number and size were determined using NMR spectroscopy (LipoScience). Plasma apoAI, apoAII and apoE levels were measured by ELISA. A detailed description of the RNA and protein analyses, as well as the HDL characterization assays, is in the Methods.

Full Methods and any associated references are available in the online version of the paper at www.nature.com/nature.

Received 20 May; accepted 17 August 2011.

1. deGoma, E. M. & Rader, D. J. Novel HDL-directed pharmacotherapeutic strategies. *Nature Rev. Cardiol.* **8,** 266–277 (2011).
2. Moore, K. J., Rayner, K. J., Suarez, Y. & Fernandez-Hernando, C. MicroRNAs and cholesterol metabolism. *Trends Endocrinol. Metab.* **21,** 699–706 (2010).
3. Marquart, T. J., Allen, R. M., Ory, D. S. & Baldan, A. miR-33 links *SREBP-2* induction to repression of sterol transporters. *Proc. Natl Acad. Sci. USA* **107,** 12228–12232 (2010).
4. Najafi-Shoushtari, S. H. *et al.* MicroRNA-33 and the SREBP host genes cooperate to control cholesterol homeostasis. *Science* **328,** 1566–1569 (2010).
5. Rayner, K. J. *et al.* miR-33 contributes to the regulation of cholesterol homeostasis. *Science* **328,** 1570–1573 (2010).
6. Rayner, K. J. *et al.* Antagonism of miR-33 in mice promotes reverse cholesterol transport and regression of atherosclerosis. *J. Clin. Invest.* **121,** 2921–2931 (2011).
7. Davalos, A. *et al.* miR-33a/b contribute to the regulation of fatty acid metabolism and insulin signaling. *Proc. Natl Acad. Sci. USA* **108,** 9232–9237 (2011).
8. Gerin, I. *et al.* Expression of miR-33 from an *SREBP2* intron inhibits cholesterol export and fatty acid oxidation. *J. Biol. Chem.* **285,** 33652–33661 (2010).
9. Horton, J. D., Goldstein, J. L. & Brown, M. S. SREBPs: activators of the complete program of cholesterol and fatty acid synthesis in the liver. *J. Clin. Invest.* **109,** 1125–1131 (2002).
10. Horie, T. *et al.* microRNA-33 encoded by an intron of sterol regulatory element-binding protein 2 (*Srebp2*) regulates HDL *in vivo*. *Proc. Natl Acad. Sci. USA* **107,** 17321–17326 (2010).
11. Geary, R. S. Antisense oligonucleotide pharmacokinetics and metabolism. *Expert Opin. Drug Metab. Toxicol.* **5,** 381–391 (2009).
12. Chyu, K. Y., Peter, A. & Shah, P. K. Progress in HDL-based therapies for atherosclerosis. *Curr. Atheroscler. Rep.* **3,** 405–412 (2011).
13. Alberti, K. G. *et al.* Harmonizing the metabolic syndrome: a joint interim statement of the International Diabetes Federation Task Force on Epidemiology and Prevention; National Heart, Lung, and Blood Institute; American Heart Association; World Heart Federation; International Atherosclerosis Society; and International Association for the Study of Obesity. *Circulation* **120,** 1640–1645 (2009).

Supplementary Information is linked to the online version of the paper at www.nature.com/nature.

Acknowledgements This work was supported by grants from the National Institutes of Health to K.J.M. (R01AG02055 and R01HL108182), E.A.F. (P01HL098055, R01HL084312 and R01HL58541), C.F.-H. (1P30HL101270 and R01HL107953), R.E.T. (R00HL088528), as well as by the Canadian Institutes of Health Research (K.J.R.)

Author Contributions K.J.M. and R.E.T. contributed equally to this study. K.J.M., R.E.T., C.C.E. and K.J.R. designed the study. C.J.L., R.E.T., A.L.M., S.M.M. and K.J.R. assisted in the necropsy. K.J.R., R.E.T., F.N.H., J.M.V.G., F.J.S., L.G. and T.D.R. performed the biological assays. C.C.E., X.L., O.G.K. and V.K. conducted the miRNA and microarray analyses. E.A.F. and C.F.-H. assisted with the experimental design and data interpretation. K.J.M. and K.J.R. wrote the first draft of the manuscript, which was commented on by all authors.

Author Information The microarray data have been deposited in the Gene Expression Omnibus database under accession number GSE31177. Reprints and permissions information is available at www.nature.com/reprints. The authors declare no competing financial interests. Readers are welcome to comment on the online version of this article at www.nature.com/nature. Correspondence and requests for materials should be addressed to K.J.M. (kathryn.moore@nyumc.org) or R.E.T. (rtemel@wfubmc.edu).

METHODS

African green monkeys. Adult male African green monkeys (*Chlorocebus aethiops*) ($n = 12$, age 5–10 years) were obtained from St. Kitts island. Monkeys were housed in an AAALAC-accredited facility under the direct care of the Wake Forest University Health Sciences (WFUHS) Animal Resources Program and necropsied at the termination of the study. All experiments were approved by the WFUHS Institutional Animal Care and Use Committee (IACUC). Monkeys were singly housed in climate-controlled conditions with a 12 h light and dark cycle.

The monkeys were provided water *ad libitum* and were initially fed a weighed amount of a chow diet (Monkey Diet 5038, Lab Diet) twice daily, such that their daily caloric intake was 70 kcal day^{-1} kg^{-1} body weight. To induce dyslipidaemia, the monkeys were fed twice daily with a weighed amount of a high carbohydrate, moderate cholesterol semisynthetic diet (Supplementary Table 3), which was prepared at the Wake Forest Primate Center Diet Laboratory, such that their daily caloric intake was 90 kcal day^{-1} kg^{-1} body weight. The use of a similar semisynthetic high-fructose diet in cynomolgus monkeys has been shown to increase plasma triglyceride levels[14].

Liver biopsy. Liver samples were collected from chow-fed monkeys before and after 4 weeks of anti-miRNA treatment. After an overnight fast, the monkeys were initially anaesthetized with ketamine (10 mg kg^{-1} intramuscularly) and pretreated with atropine (0.04 mg kg^{-1} intramuscularly). After intubation, anaesthesia was maintained throughout the surgical procedure with isoflurane (3.5–5.0% for induction, and 1–2% for maintenance, by inhalation). The monkeys were shaved and prepared for surgery in accordance with standard veterinary medical practice (three sequential scrubs with Nolvasan and rinses with isopropanol, and a final spray with Betadine solution). Anaesthesia was monitored at 15-min intervals during the surgical procedure. If there was a change after the monkeys reached the desired plane of anaesthesia, anaesthesia was increased or decreased at the direction of the surgical veterinarian. Heart rate, oxygen saturation, end expired CO_2, capillary refill time, respiration rate and temperature were recorded at 15-min intervals or more frequently if needed. Under sterile conditions, an abdominal incision was made and a 1-g wedge of liver was taken. The monkeys were administered buprenorphine HCl (0.01 mg kg^{-1} intramuscularly) for pre-emptive analgesia. The laparotomy incision was closed in a standard three-layer manner, with the abdominal wall closed using a synthetic absorbable suture in a simple interrupted pattern. The subcutis was similarly closed with a continuous suture pattern, using a synthetic absorbable material, and the skin was opposed with a continuous pattern of intradermally placed suture. The monkeys were returned to their cages and monitored during anaesthetic recovery in accordance with the WFUHS IACUC policy on survival surgery and post-surgical care. For 10 days following surgery, the monkeys were monitored for post-operative pain, which was alleviated with buprenorphine HCl (0.01 mg kg^{-1} intramuscularly, twice daily) and ketoprofen (2.0–3.0 mg kg^{-1} intramuscularly, once daily).

Anti-miRNA treatment. Regulus Therapeutics provided 2′-F/MOE-modified, phosphorothioate-backbone-modified antisense miR-33 (TGCAATGCAACTA CAATGCAC) and mismatch control (TCCAATCCAACTTCAATCATC) anti-miRNA (the mismatched bases are underlined). Monkeys were injected subcutaneously with 5 mg anti-miRNA kg^{-1} body weight twice weekly during the first 2 weeks and then once weekly during the remaining 10 weeks of the study.

Monitoring for adverse effects. To monitor for any adverse effects of anti-miRNA treatment, body weights were measured weekly. In addition, at week 0, 4, 8 and 12 of anti-miRNA treatment, analysed serum and whole blood samples were analysed by ANTECH Diagnostics, using the Superchem and CBC tests, respectively.

RNA extraction and qPCR. Liver tissue was homogenized in 300 µl TRIzol (Invitrogen) with 1-mm zirconium silicate beads, using a Bullet Blender (Next Advance). Insoluble material and the beads were removed by centrifugation; the volume of TRIzol was brought up to 1 ml; and RNA was extracted according to the manufacturer's protocol. RNA integrity was verified using Agilent's Bioanalyzer. Reverse transcription was carried out on 1 µg total RNA using the iScript cDNA Synthesis Kit (Bio-Rad). qPCR was performed using the Eppendorf Mastercycler with primers directed against the genes listed in Supplementary Table 2.

miR-33a and miR-33b detection was performed using a QuantiGene 2.0 miRNA Assay (Panomics) according to the manufacturer's instructions. Total RNA (1-mg input) was used for each liver sample. Copy number quantification was done by generating a standard curve using miR-33a and miR-33b oligonucleotides synthesized by Integrated DNA Technologies.

Affymetrix gene array analysis. Microarray analysis of liver biopsies from monkeys treated with anti-miR-33 or a control anti-miRNA were performed in groups of six, using Human U133 Plus 2.0 Arrays (Affymetrix). Treatments were performed at three time points: 0, 4 and 12 weeks. Data from the arrays were normalized, quality controlled and compared using two-way analysis of variance (ANOVA) tests. Genes with a heptamer signature seed sequence that matched miR-33 were filtered using *P* values with an $\alpha < 0.05$ and sorted by fold change. The miR-33 seed sequence was taken from miRBase (http://www.mirbase.org), and seed-matched genes were derived from genes with 3′-untranslated region (UTR) seed-sequence matches in the Ensembl BioMart database (http://www.biomart.org).

HPLC-ES/MS quantification of anti-miRNA. Anti-miRNA was quantified in liver samples by ion-pairing HPLC-ES/MS. Separation was accomplished using a 1200 series HPLC-MS system (Agilent Technologies) consisting of a binary pump, a diode array ultraviolet detector, a column oven, an autosampler and a 6100 Single Quadrupole MS. Typically, each sample (50 mg) was extracted using a phenol–chloroform–isoamyl alcohol (25:24:1) extraction method followed by a two-step solid-phase extraction method (strong anion exchange followed by reverse phase C18). The extracted material was reconstituted in water and injected directly onto an XBridge OST C18 column (50 × 2.1 mm, 2.5 mm particles; Waters). The column was maintained at 55 °C, and the flow rate on the column was 0.1 ml min^{-1}. The column was equilibrated with 25% acetonitrile in 5 mM tributylammonium acetate, pH 7.0. A gradient from 30% to 60% acetonitrile over 10 min was used to separately elute the compound of interest and the internal standard (a 27-amino acid 2′-F/MOE-modified compound). Peak areas were quantified online using single-ion monitoring mode with $m/z = 1{,}868$ for RG428651 and 1,843 for RG522293. Mass spectra were obtained using a drying gas flow rate of 12 l min^{-1} at 350 °C, a nebulizer pressure of 35 psig and a capillary voltage of 4,000 V. Chromatograms were analysed using ChemStation software. Compound levels were back-calculated using a quadratic fit and calibration curve range of 15.6–500 mg g^{-1} tissue. The lower limit of quantification (LLOQ) was equal to 31.3 mg g^{-1} tissue.

Protein extraction and western blotting analyses of liver. Liver tissue was homogenized in 500 µl RIPA buffer using a Bullet Blender, as described above. Lysates were cleared by centrifugation, and a total of 50 µg protein was separated using SDS–PAGE and transferred to nitrocellulose or polyvinylidene difluoride. Membranes were blotted with antibodies against ABCA1 (rabbit; from M. Fitzgerald[15]), CPT1A (goat; Novus Biologicals), CROT (rabbit; Abcam) and tubulin (mouse; Sigma). Secondary antibodies labelled with IRDye800 or IRDye700 (Rockland Immunochemicals for Research) were visualized using an Odyssey Imaging System (LI-COR).

Cholesterol efflux assays. THP-1 cells (1 x 10^6 per well) were differentiated in 10 nM phorbol myristate acetate for 72 h in RPMI medium supplemented with 10% FBS. Cells were loaded by incubation with 37.5 µg ml^{-1} acetylated LDL (Biomedical Technologies) and labelled with 0.5 µCi ml^{-1} [^{3}H]cholesterol (PerkinElmer) for 24 h. Excessive label was removed by extensive washing with PBS before cells were equilibrated in 2 mg ml^{-1} fatty-acid-free BSA in RPMI. To use as an acceptor in the efflux studies, HDL was isolated by combining pooled serum samples (from $n = 6$ monkeys treated with either mismatch control or anti-miR33) with 20% PEG (Sigma) followed by centrifugation, to precipitate the apoB-containing lipoproteins, as described previously[16]. The cholesterol content of this PEG-isolated HDL was determined to be 526 µg ml^{-1} for control anti-miRNA-treated monkeys and 863 µg ml^{-1} for anti-miR-33-treated monkeys. Medium containing equal volumes (25 µl) of this PEG-isolated HDL was added to the labelled cells for 6 h. Alternatively, 2.5% pooled serum from each group of monkeys was added to the cells as an efflux acceptor for 6 h. Supernatants were collected, and the ^{3}H was counted and expressed as a percentage of the total cell [^{3}H]cholesterol content (total effluxed [^{3}H]cholesterol + cell-associated [^{3}H]cholesterol). Data are expressed as mean ± s.d. of triplicate wells and represent an experimental $n = 3$.

Luciferase assays. HEK293 cells were seeded 24 h before transfection in 24-well plates. A plasmid containing the full-length 3′-UTR of ABCA1 downstream of firefly luciferase (GeneCopoeia) was transfected into cells in the presence or absence of the following vectors: pre-miR-33a, pre-miR-33b or a control miRNA (System Biosciences) along with 20 nM of either the mismatch anti-miRNA or anti-miR-33. Twenty-four hours after transfection, cells were collected, and the luciferase activity was measured using the Dual-Glo Luciferase Assay System (Promega). Firefly luciferase activity was normalized to *Renilla* luciferase activity as a control for transfection efficiency. Data are expressed relative to the ABCA1 3′-UTR activity in the presence of a control miRNA and are mean ± s.d. of triplicate samples of an experimental $n = 3$.

Plasma lipid, apolipoprotein and lipoprotein concentrations. Monkeys were sedated with ketamine (10 mg kg^{-1} intramuscularly), and blood was collected in EDTA-containing Vacutainers. Plasma was isolated by centrifugation at 1,500*g* for 30 min at 4 °C. Total plasma cholesterol and triglyceride levels were measured using a Cholesterol Reagent Set (Pointe Scientific) and Triglyceride Reagent and Free Glycerol Reagent (Sigma), respectively. The plasma lipoprotein cholesterol and triglyceride distributions were determined by online gel-filtration HPLC[17,18], using Infinity Cholesterol or Infinity Triglycerides reagent (Thermo). The plasma lipoprotein particle number and size were determined by LipoScience using NMR,

as described previously[19]. Plasma apoAI, apoAII and apoE levels were measured by ELISA[20].

Plasma cholesterol and apolipoprotein distribution. An equal volume of plasma from each monkey within a treatment group was pooled. The pooled plasma was separated on a Superose 6 10/300 GL column (GE Healthcare) at a flow rate of 0.4 ml min^{-1}. From 20 to 60 min post-injection, fractions were collected at 1-min intervals. The total cholesterol content of the fractions was determined using a Cholesterol Reagent Set (Pointe Scientific). An equal volume of each fraction was mixed with 5× SDS sample buffer and separated on a Novex NuPAGE 4–12% Bis-Tris Midi Gel using 1× NuPAGE MOPS SDS running buffer (Invitrogen). The proteins were transferred to a nitrocellulose membrane, which was subsequently blocked with 5% (w/v) non-fat dried milk dissolved in wash buffer. The membrane was incubated overnight at 4 °C in one or more of the following goat anti-monkey affinity-purified antibodies: anti-apoAI, anti-apoAII, anti-apoB or anti-apoE. All anti-monkey apolipoprotein antibodies were created and tested for specificity at WFUHS. Secondary antibodies against goat IgG were conjugated to horseradish peroxidase (Sigma), and proteins were visualized with ECL reagent (PerkinElmer) and exposure to Blue X-Ray Film (Phenix).

Plasma cytokine analysis. The levels of cytokines in plasma samples were measured using a Human Proinflammatory 7-Plex Assay Ultra-Sensitive Kit (Meso Scale Discovery). The assay was done according to the manufacturer's assay procedure. Briefly, 25 µl monkey plasma samples or kit calibrators were added to assay diluent in a 96-well 7-plex assay plate. After incubation for 2 h, the plate was washed then incubated with detection antibody solution for 2 h. Read Buffer was added to each well in the assay plate, and the signal was analysed by a SECTOR Imager (Meso Scale Discovery). Seven cytokines, including interleukin-1β (IL-1β), IL-12p70, interferon-γ, IL-6, IL-8, IL-10 and tumour-necrosis factor-α, were analysed simultaneously by the imager. The data were quantified using a standard curve generated from the kit calibrators for each of the cytokines.

Flow cytometric analysis of endothelial VCAM1 and E-selectin. Human umbilical vein endothelial cells (HUVECs; Lonza) were cultured in EGM-2 according to the manufacturer's protocol. HUVECs (passage 3–5) were plated in 24-well plates, with 1×10^5 cells in 400 µl EGM-2 containing 20% FBS per well. After a 5-h re-attachment period, cells were pre-incubated for 16 h with HDL isolated from pooled serum samples ($n = 6$), after which TNF-α (0.5 ng ml^{-1}; PeproTech) was added to the culture medium for an additional 4 h. Cell-surface expression of VCAM1 and E-selectin was then measured by flow cytometry, using an anti-VCAM1 monoclonal antibody (BD Biosciences) followed by an anti-mouse fluorescein isothiocyanate (FITC)-conjugated antibody (Sigma) or an anti-E-selectin phycoerythrin (PE)-conjugated antibody (Chemicon). Cells were detached using 5 mM EDTA in PBS. Cellular FITC and PE were then analysed by flow cytometry (with an Accuri C6 Flow Cytometer; BD Biosciences). Controls included an isotype-matched control antibody and no primary antibody. Native HDL_3 (isolated by sequential ultracentrifugation of human plasma) at a concentration of 0.5 mg ml^{-1} protein was used as a positive control.

Statistical analyses. All comparisons were made using Student's *t*-test ($P \leq 0.05$), and data are expressed as mean ± s.e.m., unless otherwise noted. Data from the arrays were normalized, quality controlled and compared using two-way ANOVA tests.

14. Wagner, J. E. *et al.* Old world nonhuman primate models of type 2 diabetes mellitus. *ILAR J.* **47,** 259–271 (2006).
15. Fitzgerald, M. L. *et al.* ATP-binding cassette transporter A1 contains an NH2-terminal signal anchor sequence that translocates the protein's first hydrophilic domain to the exoplasmic space. *J. Biol. Chem.* **276,** 15137–15145 (2001).
16. Yvan-Charvet, L. *et al.* ATP-binding cassette transporters and HDL suppress hematopoietic stem cell proliferation. *Science* **328,** 1689–1693 (2010).
17. Kieft, K. A., Bocan, T. M. A. & Krause, B. R. Rapid on-line determination of cholesterol distribution among plasma lipoproteins after high-performance gel filtration chromatography. *J. Lipid Res.* **32,** 859–866 (1991).
18. Garber, D. W., Kulkarni, K. R. & Anantharamaiah, G. M. A sensitive and convenient method for lipoprotein profile analysis of individual mouse plasma samples. *J. Lipid Res.* **41,** 1020–1026 (2000).
19. Jeyarajah, E. J., Cromwell, W. C. & Otvos, J. D. Lipoprotein particle analysis by nuclear magnetic resonance spectroscopy. *Clin. Lab. Med.* **26,** 847–870 (2006).
20. Koritnik, D. L. & Rudel, L. L. Measurement of apolipoprotein A-I concentration in nonhuman primate serum by enzyme-linked immunosorbent assay (ELISA). *J. Lipid Res.* **24,** 1639–1645 (1983).